JOURNAL OF VIROLOGY, Feb. 2005, p. 2079–2086 Vol. 79, No. 4
0022-538X/05/$08.00+0 doi:10.1128/JVI.79.4.2079–2086.2005

Inhibition of Beta Interferon Induction by Severe Acute Respiratory Syndrome Coronavirus Suggests a Two-Step Model for Activation of Interferon Regulatory Factor 3

Martin Spiegel,[1] Andreas Pichlmair,[1] Luis Martínez-Sobrido,[2] Jerome Cros,[2] Adolfo García-Sastre,[2] Otto Haller,[1] and Friedemann Weber[1]*

Abteilung Virologie, Institut für Medizinische Mikrobiologie und Hygiene, Universität Freiburg, Freiburg, Germany,[1] *and Department of Microbiology, Mount Sinai School of Medicine, New York, New York*[2]

Received 7 June 2004/Accepted 20 September 2004

Severe acute respiratory syndrome (SARS) is caused by a novel coronavirus termed SARS-CoV. We and others have previously shown that the replication of SARS-CoV can be suppressed by exogenously added interferon (IFN), a cytokine which is normally synthesized by cells as a reaction to virus infection. Here, we demonstrate that SARS-CoV escapes IFN-mediated growth inhibition by preventing the induction of IFN-β. In SARS-CoV-infected cells, no endogenous IFN-β transcripts and no IFN-β promoter activity were detected. Nevertheless, the transcription factor interferon regulatory factor 3 (IRF-3), which is essential for IFN-β promoter activity, was transported from the cytoplasm to the nucleus early after infection with SARS-CoV. However, at a later time point in infection, IRF-3 was again localized in the cytoplasm. By contrast, IRF-3 remained in the nucleus of cells infected with the IFN-inducing control virus Bunyamwera delNSs. Other signs of IRF-3 activation such as hyperphosphorylation, homodimer formation, and recruitment of the coactivator CREB-binding protein (CBP) were found late after infection with the control virus but not with SARS-CoV. Our data suggest that nuclear transport of IRF-3 is an immediate-early reaction to virus infection and may precede its hyperphosphorylation, homodimer formation, and binding to CBP. In order to escape activation of the IFN system, SARS-CoV appears to block a step after the early nuclear transport of IRF-3.

Severe acute respiratory syndrome (SARS) is a life-threatening form of atypical pneumonia which has recently emerged as a new human disease, resulting in over 8,000 cases and 774 deaths in 30 countries (9, 49, 69). A novel virus, termed SARS coronavirus (SARS-CoV), was isolated from patients and identified as the etiologic agent (15, 18, 33, 34, 48).

Virus infection of mammalian cells prompts the innate immune system to mount a first line of defense. Infected cells synthesize and secrete alpha/beta interferons (IFN-α/β), which cause neighboring cells to express antiviral factors, thereby limiting viral spread (60). In tissue cells, transcription of the IFN-β gene represents the primary response to virus infection (13, 16, 44). Induction of the IFN-β gene requires the constitutively expressed transcription factor interferon regulatory factor 3 (IRF-3) (40, 54, 65, 66, 72). In uninfected cells, IRF-3 is inactive and resides in the cytoplasm. The current model of IRF-3 activation proposes a sequence of events beginning with phosphorylation by a virus-activated kinase (17, 58). Phosphorylated IRF-3 then homodimerizes and is translocated into the nucleus, where it recruits the transcriptional coactivator CREB-binding protein (CBP), to initiate IFN-β mRNA synthesis (27, 61). Once secreted, IFN-β binds to its receptor on the cell surface and activates the synthesis of proteins with antiviral, antiproliferative, and immunomodulatory properties (12). IFN-β also participates in the induction of IFN-αs, which further amplify the antiviral response (13, 16, 44).

Viruses have evolved effective strategies to evade the interferon system (23, 37, 68). They can inhibit IFN induction, IFN signal transduction, or the action of particular antiviral proteins by various mechanisms, including double-stranded RNA binding and IRF-3 sequestration.

SARS-CoV is known to be sensitive to the antiviral action of IFNs, because its growth in tissue culture is efficiently inhibited by exogenously added IFN-β, and, less efficiently, also by IFN-α (11, 24, 59). Furthermore, treatment with IFN-α can protect experimentally infected macaques (24) and may alleviate symptoms in SARS patients (41). We therefore considered whether SARS-CoV may be able to circumvent IFN induction in order to avoid IFN-mediated growth inhibition. Here, we evaluated this hypothesis by investigating IFN-β transcription and activation of IRF-3 in cells infected with SARS-CoV.

MATERIALS AND METHODS

Cells and viruses. Simian VeroE6 cells and human 293 cells were maintained and grown as previously described (59). The FFM-1 isolate of SARS-CoV was kindly provided by Stephan Becker, University of Marburg, Germany. Bunyamwera delNSs virus (67) was used as an IFN-inducing control virus.

Generation of antibodies. Monoclonal antibodies against human IRF-3 were generated by immunizing mice with a bacterially expressed glutathione *S*-transferase fusion protein containing the C-terminal 100 amino acids (328 to 427) of human IRF-3. Hybridomas were screened on 96-well plates coated with bacterially expressed full-length human IRF-3 protein, and two specific monoclonal antibodies (17C2 and 6C7) were obtained. To generate a polyclonal antiserum against SARS-CoV, the N cDNA sequence (Urbani strain) was amplified by reverse transcription-PCR, with RNA from infected Vero cells as the template. Primer sequences were 5′-CCGGGAATTCACCATGTCTGATAATGGACCCCAATCA-3′ and 5′-GCGCGCATGCTTATGCCTGAGTTGAATCAGCAGA-3′. The reverse transcription-PCR product was cloned into pET28a (Novagene)

* Corresponding author. Mailing address: Abteilung Virologie, Institut für Medizinische Mikrobiologie und Hygiene, Universität Freiburg, D-79008 Freiburg, Germany. Phone: 49-761-203-6614. Fax: 49-761-203-6562. E-mail: friedemann.weber@uniklinik-freiburg.de.

with EcoRI and XhoI restriction sites. pET28a/N was transformed into *Escherichia coli* strain BL21(DE3) to produce recombinant N protein. After purification by Ni-nitrilotriacetic acid-agarose beads (Qiagen), a rabbit was immunized and serum was collected after two boosts (Cocalico Biologicals Inc., Reamstown, Pa.). The specificity of all sera was tested by immunofluorescence and Western blot analysis.

IFN reporter assays. Subconfluent 293 cells were transfected with 0.5 μg of the IFN-β promoter reporter construct p-125Luc (kindly provided by Takashi Fujita, Tokyo Metropolitan Institute of Medical Science, Tokyo, Japan) and 0.05 μg of control plasmid pRL-SV40 (Promega) mixed with 2.5 μl of DAC-30 (Eurogentec) in 200 μl of Optimem (Gibco-BRL). After 6 h at 37°C, the liposome-DNA mixture was removed, and cells were infected at a multiplicity of infection of 5. At 18 h postinfection, cells were harvested and lysed in 100 μl of passive lysis buffer (Promega). An aliquot of 20 μl of lysate was used to measure firefly and *Renilla* luciferase activities according to the manufacturer's instructions. The firefly luciferase activities were normalized to the corresponding *Renilla* luciferase activities to determine induction.

Reverse transcription-PCR analyses. Cells were infected for 18 h and total RNA was extracted. For reverse transcription, 1 μg of RNA was incubated with 200 U of Superscript II reverse transcriptase (Gibco-BRL) and 100 ng of random hexanucleotides in 20 μl of 1× reverse transcription buffer (Gibco-BRL) supplied with 1 mM each of the four deoxynucleotide triphosphates, 20 U of RNasin, and 10 mM dithiothreitol. The resulting cDNA was amplified by 35 cycles of PCR, with each cycle consisting of 30 s at 94°C, 1 min at 58°C, and 1 min at 72°C, followed by 10 min at 72°C. The upstream and downstream primers for amplifying mRNA sequences were 5′-GACGCCGCATTGACCATCTA-3′ and 5′-CCTTAGGATTTCCACTCTGACT-3′ (IFN-β), 5′-ATGTCTGATAATGGACCCCAATCAAACCAA-3′ and 5′-TTATGCCTGAGTTGAATCAGCAGAAGCTCCA-3′ (SARS-CoV N), 5′-ATGATTGAGTTGGAATTTCATGAT-3′ and 5′-CCCTGCTTACATGTTGATTCCGAATTTAGCAA-3′ (Bunyamwera virus N), and 5′-GCCGGTCGCAATGGAAGAAGA-3′ and 5′-CATGGCCGGGGTGTTGAAGGTC-3′ (γ-actin).

IRF-3 nuclear translocation assay. Endogenous IRF-3 can be detected in Vero cells by enzymatic amplification of the immunofluorescence signal (32). Cells were grown on coverslips and infected with SARS-CoV at a multiplicity of infection of 5. After an incubation period of 8 h or 16 h, cells were fixed with 3% paraformaldehyde and permeabilized with 0.5% Triton X-100 dissolved in phosphate-buffered saline (PBS). Cells were washed three times with PBS and incubated with the primary antibodies, polyclonal rabbit anti-SARS-CoV N protein and monoclonal mouse anti-IRF-3 antibody 17C2, diluted 1:1,000 and 1:500, respectively, in TNB blocking buffer (Perkin Elmer). After incubation at room temperature for 1 h, the coverslips were washed three times in PBS and then treated with the secondary antibodies, Cy3-conjugated goat anti-rabbit immunoglobulin G (Alexis) and biotin-conjugated anti-mouse immunoglobulin (Perkin Elmer) at a dilution of 1:200 each. Cells were again washed three times in PBS and incubated for 30 min with streptavidin-conjugated horseradish peroxidase (Perkin Elmer) at a dilution of 1:100. After washing in PBS, cells were incubated for 5 min in Fluorophore Tyramide amplification reagent (Perkin Elmer), then washed in PBS, and mounted with Fluorsave solution (Calbiochem). Stained cell samples were examined with a Leica confocal laser scanning microscope with an ×63 NA1.4 objective.

IRF-3 hyperphosphorylation assay. Cells were lysed in radioimmunoprecipitation assay (RIPA) buffer (50 mM Tris, pH 7.6, 150 mM NaCl, 1% NP-40) containing protease inhibitors (Complete protease inhibitor; Roche) and phosphatase inhibitors (phosphatase inhibitor cocktail II; Calbiochem). A total of 50 μg of protein was separated by electrophoresis on a 5% to 12% polyacrylamide gradient gel and blotted onto an Immobilon-P membrane (Millipore) following the manufacturer's instructions (Bio-Rad). The membrane was incubated with a 1:500 dilution of polyclonal anti-IRF-3 antibody FL-425 (Santa Cruz Biotechnology). Protein bands were visualized with the ECL Plus method (Amersham).

IRF-3 dimerization assay. Cells were lysed in buffer containing 50 mM Tris-HCl (pH 7.5), 150 mM NaCl, 1 mM EDTA, 1% NP-40, protease inhibitors, and phosphatase inhibitors, vortexed, incubated on ice for 10 min, and then centrifuged at 4°C for 5 min at 10,000 × *g*. Proteins were then separated by electrophoresis in a 10% nondenaturing polyacrylamide gel, with 1% deoxycholate in the cathode buffer (29). IRF-3 monomers and dimers were detected by Western blot analysis with polyclonal anti-IRF-3 antibody FL-425 (Santa Cruz Biotechnology) diluted 1:500.

Coimmunoprecipitation assay. Human 293 cells (2×10^6) were grown to 80% confluency and infected with SARS-CoV at a multiplicity of infection of 5. After an incubation period, cells were washed in PBS and incubated in 200 μl of RIPA buffer containing protease and phosphatase inhibitors. In parallel, 30 μl of a 50% slurry of protein G-Sepharose in RIPA buffer were preadsorbed with 2 μg of polyclonal anti-CBP antibody A-22 (Santa Cruz Biotechnology) and incubated for 2 h at 4°C. Then, the Sepharose beads were washed three times with RIPA buffer and incubated with the cell lysate for 2 h at 4°C. The immunoprecipitates were washed three times with RIPA buffer, and bound proteins were subjected to Western blot analysis with the mouse monoclonal anti-IRF-3 antibody SL12 (Pharmingen), diluted 1:500, or the anti-CBP antibody A-22, diluted 1:200. As infection controls, supernatants from the first precipitation step were analyzed by Western blot with rabbit polyclonal serum against SARS-CoV N protein (1:2,000) or Bunyamwera virus N (1:500).

Nuclear localization assays. The human IRF-2 cDNA was amplified from HeLa cell total RNA by reverse transcription-PCR with oligo(dT) primers for reverse transcription and primers hIRF-2/ClaI/5′ (CGCGATCGATACCATGCCGGTGGAAAGGATGCGC) and hIRF-2/KpnI/3′ (CGCGGGTACCTTAACAGCTCTTGACGCGGGC) for PCR. The PCR product was cloned into the pEGFP-C1 expression plasmid (Clontech) with ClaI and KpnI restriction enzymes. The resulting plasmid, termed pEGFP-C1-hIRF-2, expresses the green fluorescent protein (GFP) fused to IRF-2. Vero cells were transfected with 2 μg of pEGFP-C1-hIRF-2 with DAC-30 liposomes as described above. After 24 h at 37°C, cells were infected with a multiplicity of infection of 5, and 16 h postinfection, cells were immunostained for SARS-CoV N protein as indicated. Cell samples were examined with a Leica confocal laser scanning microscope with an ×63 NA1.4 objective.

Nuclear export assays. Vero cells were transfected with 850 ng of the Rev expression construct pcRev, 100 ng of the reporter plasmid pDM128 (19), and 50 ng of the control plasmid pRL-SV40 (Promega) expressing *Renilla* luciferase. pDM128 generates a chloramphenicol acetyltransferase (CAT) mRNA which is only functional if exported out of the nucleus by Rev in an unspliced form. After 4 h at 37°C, transfected cells were infected with a multiplicity of infection of 5, and 16 h postinfection, cells were harvested and lysed in 100 μl of passive lysis buffer (Promega). An aliquot of 20 μl of lysate was used to measure CAT (Roche) and *Renilla* luciferase (Promega) activities according to the manufacturers' instructions. The CAT activities were normalized to the corresponding *Renilla* luciferase activities to determine induction.

RESULTS

SARS-CoV does not induce beta interferon. To investigate induction of IFN-β, we took advantage of a human 293 cell clone which can be productively infected with SARS-CoV (data not shown). Transactivation of the IFN-β promoter was first evaluated in a luciferase reporter assay. Cells were transfected with the reporter plasmid and were then infected either with SARS-CoV or the IFN-inducing control virus Bunyamwera delNSs (67). Mock-infected cells served as a negative control. Surprisingly, SARS-CoV was unable to activate the transfected IFN-β promoter, whereas the control virus was a strong inducer, as expected (Fig. 1a).

To investigate the inducibility of the endogenous IFN-β promoter, we analyzed infected cells for the presence of IFN-β mRNA with reverse transcription-PCR. In control-infected cells, a clear IFN-β mRNA-specific signal was detected (Fig. 1b, panel 1). In contrast, no signal was detectable in cells infected with SARS-CoV, although both the control virus and SARS-CoV replicated well, as assessed by reverse transcription-PCR analysis detecting viral nucleocapsid protein (N) mRNAs (Fig. 1b, panels 2 and 3). The reverse transcription-PCR signal specific for the cellular γ-actin mRNA indicated that all preparations contained similar amounts of RNA (Fig. 1b, panel 4). Taken together, our results suggest that SARS-CoV has an intrinsic ability to prevent induction of IFN in infected cells.

Transient activation of IRF-3 nuclear transport in SARS-CoV-infected cells. The transcription factor IRF-3 normally resides in the cytoplasm. Immediately after virus infection, it becomes activated and moves to the nucleus to induce IFN-β gene transcription (35, 72). We investigated the subcellular

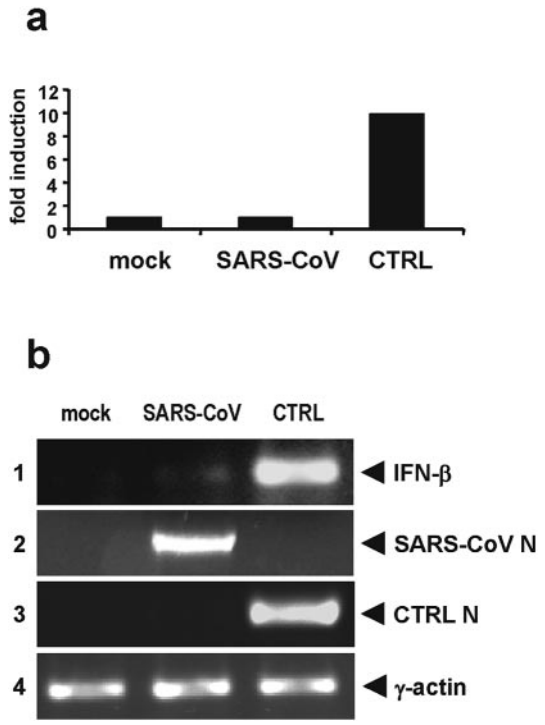

FIG. 1. Absence of IFN-β induction in SARS-CoV-infected cells. (a) IFN-β promoter activation. Human 293 cells were transfected with plasmid p-125Luc containing the firefly luciferase gene under control of the IFN-β promoter, along with a control plasmid encoding *Renilla* luciferase under control of the constitutively active simian virus 40 promoter. At 6 h posttransfection, cells were infected with SARS-CoV or the IFN-inducing control virus Bunyamwera delNSs (CTRL) or left uninfected (mock). At 18 h postinfection, luciferase activities were measured. Firefly luciferase values (reflecting IFN-β promoter activation) were normalized to the *Renilla* luciferase activities. (b) Reverse transcription-PCR analysis. Total RNA from 293 cells which were infected for 18 h was assayed by reverse transcription-PCR for the presence of IFN-β mRNA (panel 1), mRNA of the N gene of SARS-CoV (panel 2) or the control virus (panel 3), or cellular γ-actin mRNA (panel 4).

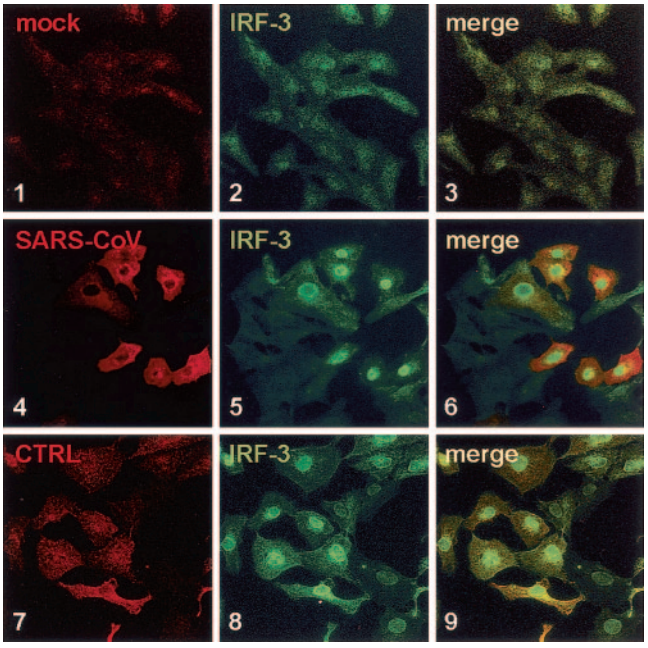

FIG. 2. Subcellular localization of IRF-3 early in infection. Confocal double immunofluorescence pictures of cells which were either mock infected (panels 1 to 3) or infected for 8 h with SARS-CoV (panels 4 to 6) or the control virus (panels 7 to 9). Viral N proteins (panels 4 and 7) and IRF-3 (panels 2, 5, and 8) were detected with specific rabbit and mouse antisera, respectively.

localization of IRF-3 in cells that were infected with SARS-CoV with immunofluorescence analysis. At 8 h after infection, IRF-3 and viral antigens were detected by double labeling with specific antibodies. In uninfected cells, no specific nuclear accumulation of IRF-3 was observed, as expected (Fig. 2, panels 1 to 3). In cells infected with SARS-CoV, IRF-3 was found in the nucleus (Fig. 2, panels 4 to 6), exactly as in cells infected with the control virus (Fig. 2, panels 7 to 9). Obviously, infection with SARS-CoV induced the nuclear transport of IRF-3 but did not lead to IFN synthesis. We therefore investigated the fate of IRF-3 at a later time point of infection. Surprisingly, in cells infected for 16 h, IRF-3 was found in the cytoplasm again (Fig. 3, panels 4 to 6), similar to uninfected cells (Fig. 3, panels 1 to 3). In contrast, IRF-3 was still in the nucleus in cells infected with the control virus (Fig. 3, panels 7 to 9). Thus, SARS-CoV infection seems to result in an early but transient nuclear accumulation of IRF-3 which is reverted at later time points.

IRF-3 hyperphosphorylation, homodimerization, and recruitment of CBP. Since SARS-CoV can block IFN-β transcription despite the observed early induction of IRF-3 nuclear translocation, we investigated whether other steps in IRF-3 activation were affected, such as hyperphosphorylation, homodimer formation, or recruitment of the coactivator protein

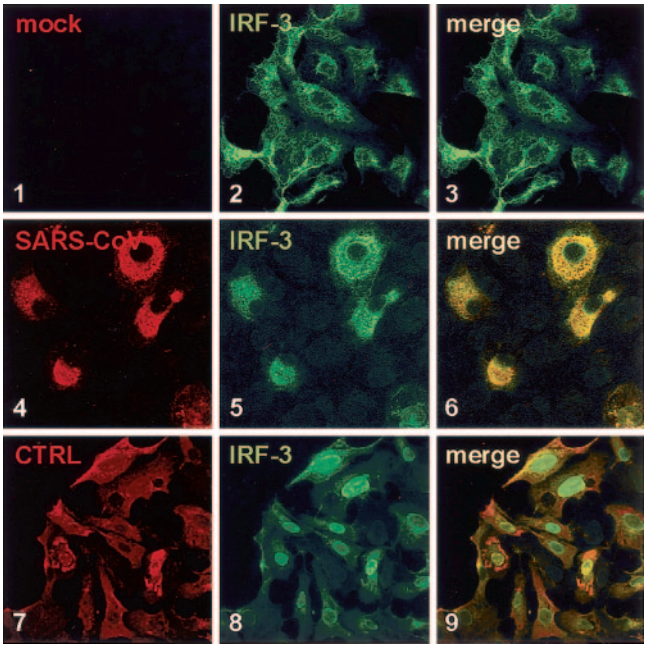

FIG. 3. Subcellular localization of IRF-3 late in infection. Cells were infected for 16 h and immunostained as indicated for Fig. 2.

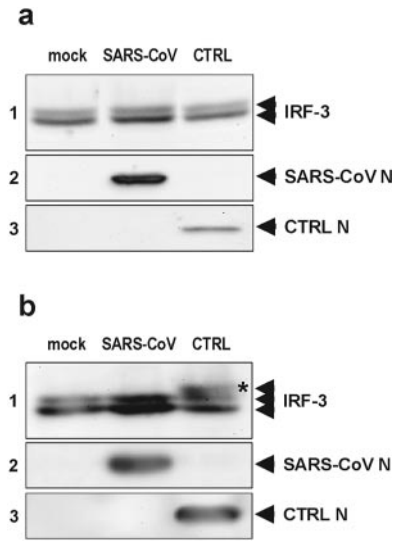

FIG. 4. Hyperphosphorylation of IRF-3. Extracts from cells infected for 8 h (a) or 16 h (b) were analyzed by sodium dodecyl sulfate gel electrophoresis, followed by immunoblot analyses to detect IRF-3 (panels 1), the N protein of SARS-CoV (panels 2), or the N protein of the control virus (panels 3). The two forms of unphosphorylated IRF-3 are indicated by arrowheads, and the hyperphosphorylated form of IRF-3 is indicated by an asterisk (*).

CBP. IRF-3 is phosphorylated at several serine residues in response to virus infection (45, 56, 72). Since hyperphosphorylated IRF-3 migrates slower in sodium dodecyl sulfate-polyacrylamide gel electrophoresis, it can be distinguished from the unphosphorylated form (40, 66, 72).

We examined the phosphorylation status of IRF-3 in response to SARS-CoV with gradient gel electrophoresis coupled to Western blot analysis. Cells were infected with either SARS-CoV or the control IFN-inducing virus or left uninfected and lysed at 8 h and 16 h postinfection. Surprisingly, no hyperphosphorylation was detectable early after infection (Fig. 4a, panel 1), although both viruses replicated to detectable levels (Fig. 4a, panels 2 and 3). At the late time point, no hyperphosphorylation of IRF-3 was detectable in SARS-CoV-infected cells, whereas the control virus induced IRF-3 hyperphosphorylation, as expected (Fig. 4b). Additional treatment with calf intestinal phosphatase (40) revealed that phosphorylation was indeed responsible for the slower-migrating form of IRF-3 (data not shown).

To examine IRF-3 homodimerization, we used nondenaturing polyacrylamide gel electrophoresis coupled to Western blot analysis (29). At the early time point of infection, neither the control virus nor SARS-CoV induced the appearance of a high-molecular-weight IRF-3 band which represents the homodimer (Fig. 5a). At the late time point, the control virus but not SARS-CoV induced IRF-3 homodimer formation (Fig. 5b).

Recruitment of the coactivator protein CBP is important for transcriptional activity of IRF-3. With a coimmunoprecipitation assay (40), we investigated the CBP-binding capacity of IRF-3 at early and late time points of infection. Figure 6a (panel 1) shows that, early in infection, neither the control virus nor SARS-CoV induced the binding of IRF-3 to CBP. At

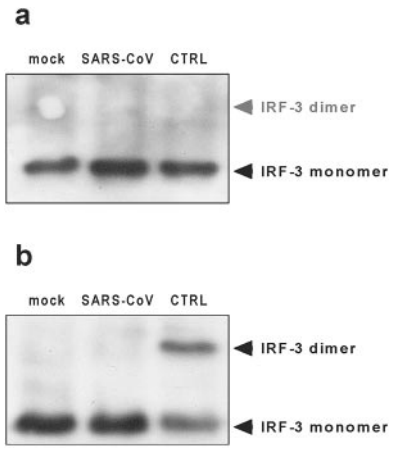

FIG. 5. Homodimerization of IRF-3. Extracts from cells infected with SARS-CoV or the control virus for 8 h (a) or 16 h (b) were analyzed by nondenaturing gel electrophoresis followed by an immunoblot to detect IRF-3. The positions of IRF-3 monomers and dimers are indicated by arrowheads.

the late time point, the CBP-IRF-3 complex was formed in cells infected with the control virus, whereas with SARS-CoV no complex formation was detectable (Fig. 6b, panel 1). Nevertheless, comparable amounts of CBP were precipitated from the lysates (Fig. 6a and b, panels 2) and infection efficiencies were comparable, as demonstrated by Western blot analyses with N-specific antibodies (Fig. 6a and b, panels 3 and 4).

Taken together, our data indicate that SARS-CoV as well as an IFN-inducing control virus activate the nuclear transport of

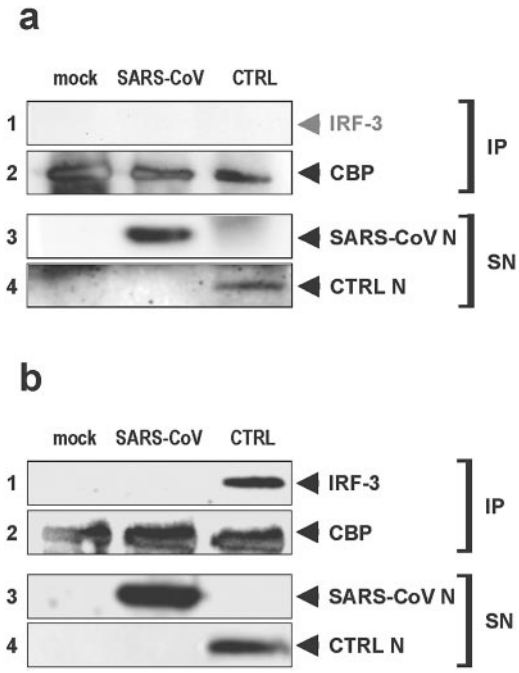

FIG. 6. CBP recruitment by IRF-3. Cells were infected for 8 h (a) or 16 h (b), and anti-CBP immunocomplexes (IP) were analyzed for the presence of IRF-3 (panels 1) and CBP (panels 2). Infections were monitored by probing the postprecipitation supernatants (SN) for the viral N proteins (panels 3 and 4).

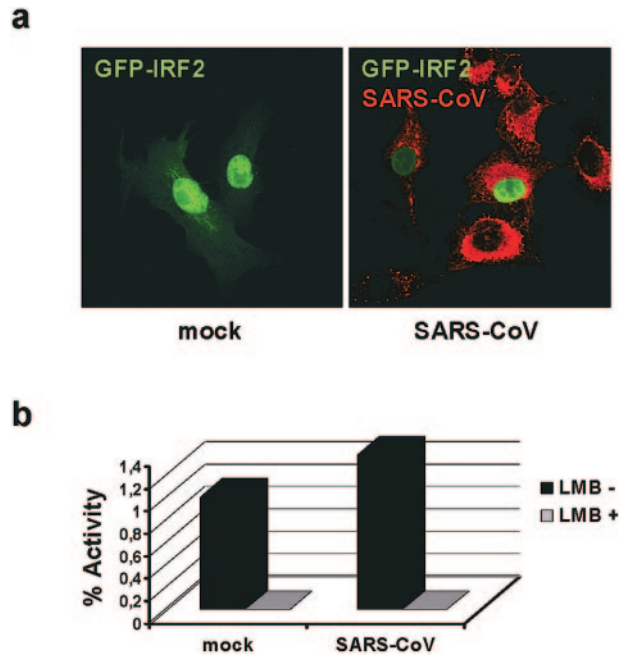

FIG. 7. Nuclear import and export. (a) Nuclear localization of IRF-2. Cells were transfected with plasmid pEGFP-C1-hIRF-2 for 24 h and then superinfected with SARS-CoV for 16 h (right panel) or left uninfected (left panel). Viral N protein was detected with a specific rabbit antiserum and a Cy3-conjugated secondary antibody. (b) Nuclear export assays. Cells were transfected with the Rev expression construct pcRev, the Rev export-dependent CAT reporter plasmid pDM128 (19), and the *Renilla* luciferase control plasmid pRL-SV40. After 4 h at 37°C, cells were either infected with SARS-CoV or left uninfected (black columns). As a control, cells were treated in parallel with the CRM-1 inhibitor leptomycin B (LMB) at a concentration of 2 ng/ml (grey columns). At 16 h postinfection, reporter activities were measured. CAT activities were normalized to the corresponding *Renilla* luciferase activities to determine induction. Data from a representative experiment are shown.

IRF-3 at early times postinfection, before detectable IRF-3 hyperphosphorylation, homodimerization, or recruitment of the coactivator CBP occurs. Subsequent to IRF-3 nuclear translocation, IRF-3 becomes fully activated and transcriptionally active in cells infected with the IFN-inducing virus but not in SARS-CoV-infected cells. Consequently, the IFN-β gene is not transcribed after SARS-CoV infection, and IRF-3, being a shuttling protein (35), localizes back to the cytoplasm later in infection.

SARS-CoV does not affect nuclear import or export. We wondered whether SARS-CoV generally affects the subcellular localization of cellular proteins. To investigate the influence on nuclear import, we transfected cells with a GFP fusion construct expressing IRF-2, a nuclear homolog of IRF-3, and infected them with SARS-CoV. In Fig. 7a (left panel) it is shown that in uninfected cells, GFP-IRF-2 localized to the nucleus, as expected. Similarly, GFP-IRF-2 was still located exclusively in the nucleus when the transfected cells were superinfected with SARS-CoV (Fig. 7a, right panel). Similar results were obtained with IRF-1, another IRF family member which localizes to the nucleus, and NLS-MxA, a cytoplasmic protein artificially fused to a nuclear localization sequence (data not shown). This indicates that SARS-CoV does not manipulate the nuclear import of cellular proteins, even if they are related to IRF-3.

The nuclear localization of IRF-3 during the early phase of infection may be caused by a block in nuclear export, trapping the shuttling protein IRF-3 in the nucleus. Nuclear export of IRF-3 is mediated by the adaptor protein CRM1 (35). To test the influence of SARS-CoV on CRM1-dependent nuclear export, we used a reporter system which measures the capacity of the human immunodeficiency virus type 1 Rev protein to export CAT mRNAs out of the nucleus (19). A second reporter construct, generating an mRNA for *Renilla* luciferase, which is exported independently of Rev/CRM1, served as an internal control. Cells were transfected with the reporter plasmids and the Rev expression construct and infected with SARS-CoV, and reporter activities were measured at 16 h postinfection. The normalized data shown in Fig. 7b demonstrate that SARS-CoV has no specific influence on CRM1-dependent nuclear export, whereas the specific CRM1 inhibitor leptomycin B strongly downregulated reporter expression, as expected. Thus, taken together, our data suggest that the transient and incomplete activation of IRF-3 by SARS-CoV in not based on a general inhibition of nuclear transport events.

DISCUSSION

Here, we demonstrate that SARS-CoV has the ability to counteract the IFN system. SARS-CoV is shown to be an inefficient IFN-β inducer, in sharp contrast to other coronaviruses (5, 10). This unique property prevents early activation of the innate immune system and may contribute to the highly pathogenic potential of the virus.

IFNs are active against most viruses (37, 53), including coronaviruses (1, 11, 20, 24, 31, 46, 59). Pathogenic viruses evolved various mechanisms to downregulate the IFN system, interfering either with IFN induction, IFN signaling, or the action of IFN-induced effector proteins (23, 37). It is becoming increasingly clear that blocking IFN induction is a most efficient and widespread mechanism to increase virus virulence (3, 68). IFN gene expression requires double-stranded RNA-induced activation of IRF-3, which, together with CBP, initiates IFN-β transcription (39, 66, 72). Viral proteins with IFN-antagonistic activity can interfere with any of these steps. Prominent examples are the NS1 protein of influenza A virus (21, 22, 42), the E3L protein of poxviruses (70), and the σ3 protein of reoviruses (28), which are double-stranded RNA-binding proteins.

Direct inhibition of IRF-3 can be achieved either through blocking of IRF-3 phosphorylation (4, 7), dominant-negative interference with IRF function by viral homologues (38, 43, 73), binding to IRF-3 (51), or sequestration of the coactivator CBP (30). Some bunyaviruses such as Rift Valley fever virus and Bunyamwera virus block IFN gene expression by targeting components of the cellular RNA polymerase II (6, 8, 36, 63, 67). Paramyxoviruses (26, 50), pestiviruses (2, 52, 55), thogotovirus (25), and picornaviruses (64, 74) are also able to block IFN production in infected cells. Our results suggest that SARS-CoV specifically interferes with IRF-3 function to prevent activation of the innate immune system. SARS-CoV apparently blocks a molecular step which is situated between the nuclear transport of IRF-3 and its subsequent activation by hyperphosphorylation and dimerization. Most probably, the

lack of stable IRF-3 dimers in SARS-CoV-infected cells prevents the recruitment of the nuclear protein CBP. It is well known that only the holocomplex consisting of an IRF-3 dimer and CBP has the ability to recognize and activate the IFN-β promoter (39, 66, 72).

To our knowledge, such a mechanism has not yet been described, suggesting that SARS-CoV uses a unique strategy for circumventing IFN induction. In addition, our data demonstrate that nuclear translocation is an early event in IRF-3 activation and precedes and occurs independently of subsequent hyperphosphorylation and homodimerization. Surprisingly, even for the IFN-inducing control virus, IRF-3 was first transported to the nucleus without apparent signs of hyperphosphorylation, homodimerization, or CBP binding. Only later in infection were these features of transcriptionally active IRF-3 detectable. This contrasts with the current model, in which hyperphosphorylation and dimerization of activated IRF-3 occur in the cytoplasm and are a prerequisite for nuclear import (57, 61). Moreover, it was postulated that IRF-3 is a shuttling protein and must be retained in the nucleus by binding to CBP (35). Our results indicate that IRF-3 can localize to the nucleus in the absence of CBP binding. Stable nuclear localization, however, correlated with hyperphosphorylation, homodimerization, and CBP binding.

We therefore favor a two-step model in which nuclear import of IRF-3 is the first and immediate response to virus infection, while hyperphosphorylation is part of a delayed response and necessary for transactivation by IRF-3. SARS-CoV appears to avoid transcription of the IFN-β gene by allowing the first step but blocking the subsequent ones. In the case of complete activation, IRF-3 hyperphosphorylation may take place either in the nucleus, or, since it is a shuttling protein, in the cytoplasm, with subsequent nuclear translocation. It might also be possible that limited phosphorylation, not detectable by sodium dodecyl sulfate-polyacrylamide gel retardation, triggers nuclear localization of IRF-3, followed by full phosphorylation and transcriptional activation.

The exact mechanism of SARS-CoV blocking of IRF-3 activation is presently unknown. Our further investigations will focus on the mechanism of action, e.g., inhibition of the IRF-3 kinases TBK1 and IKKε (17, 58) or their upstream signaling molecule, the double-stranded RNA sensor protein RIG-I (71). In addition, experiments are under way to identify the viral protein responsible for the IFN-antagonistic effect.

SARS proceeds rapidly and follows a multistep pattern with an initial, febrile stage representing exponential virus growth and spread to different organs. Later stages are characterized by immunoglobulin G seroconversion, a decrease in viral load, and clinical complications (47, 62). In SARS victims, lung tissues as well as lymphatic organs are severely damaged, and viral inclusions can be detected (14). Our data provide a plausible explanation for the rapid progression of SARS. Apparently, SARS-CoV circumvents the innate immune system by suppressing the induction of IFN, buying time to spread during the initial phase of infection. Identifying the underlying virulence mechanisms may be helpful for the rational design of specific antiviral therapies and engineering of attenuated vaccines.

ACKNOWLEDGMENTS

We thank Stephan Becker from the University of Marburg for the generous gift of SARS-CoV isolate FFM-1 and Alla Pritsker at Mount Sinai Hybridoma Center for generating the monoclonal antibodies. We also acknowledge Richard Cádagan for excellent technical assistance and Jason Paragas for sharing reagents.

This work was supported by the grants GZ Nr. 239 (202/12) from the Sino-German Center for Research Promotion and We 2616/4 from the Deutsche Forschungsgemeinschaft (F.W.), grant Ha 1582/4 from the Deutsche Forschungsgemeinschaft (O.H.), and grants from the National Institutes of Health (A.G.-S.).

ADDENDUM IN PROOF

While this paper was under review, a two-step activation mechanism for IRF-3 was described by S. N. Sarkar, K. L. Peters, C. P. Elco, S. Sakamoto, S. Pal, and G. C. Sen (Nat. Struct. Mol. Biol. **11:**1060–1067).

REFERENCES

1. **Aurisicchio, L., P. Delmastro, V. Salucci, O. G. Paz, P. Rovere, G. Ciliberto, N. La Monica, and F. Palombo.** 2000. Liver-specific alpha 2 interferon gene expression results in protection from induced hepatitis. J. Virol. **74:**4816–4823.
2. **Baigent, S. J., G. Zhang, M. D. Fray, H. Flick-Smith, S. Goodbourn, and J. W. McCauley.** 2002. Inhibition of β interferon transcription by noncytopathogenic bovine viral diarrhea virus is through an interferon regulatory factor 3-dependent mechanism. J. Virol. **76:**8979–8988.
3. **Basler, C. F., and A. Garcia-Sastre.** 2002. Viruses and the type I interferon antiviral system: induction and evasion. Int. Rev. Immunol. **21:**305–337.
4. **Basler, C. F., A. Mikulasova, L. Martinez-Sobrido, J. Paragas, E. Muhlberger, M. Bray, H. D. Klenk, P. Palese, and A. Garcia-Sastre.** 2003. The Ebola virus VP35 protein inhibits activation of interferon regulatory factor 3. J. Virol. **77:**7945–7956.
5. **Baudoux, P., L. Besnardeau, C. Carrat, P. Rottier, B. Charley, and H. Laude.** 1998. Interferon alpha inducing property of coronavirus particles and pseudoparticles. Adv. Exp. Med. Biol. **440:**377–386.
6. **Billecocq, A., M. Spiegel, P. Vialat, A. Kohl, F. Weber, M. Bouloy, and O. Haller.** 2004. NSs protein of Rift Valley fever virus blocks interferon production by inhibiting host gene transcription. J. Virol. **78:**9798–9806.
7. **Bossert, B., S. Marozin, and K. K. Conzelmann.** 2003. Nonstructural proteins NS1 and NS2 of bovine respiratory syncytial virus block activation of interferon regulatory factor 3. J. Virol. **77:**8661–8668.
8. **Bouloy, M., C. Janzen, P. Vialat, H. Khun, J. Pavlovic, M. Huerre, and O. Haller.** 2001. Genetic evidence for an interferon-antagonistic function of Rift Valley fever virus nonstructural protein NSs. J. Virol. **75:**1371–1377.
9. **Chan, H. L., S. K. Tsui, and J. J. Sung.** 2003. Coronavirus in severe acute respiratory syndrome (SARS). Trends Mol. Med. **9:**323–325.
10. **Charley, B., and H. Laude.** 1988. Induction of alpha interferon by transmissible gastroenteritis coronavirus: role of transmembrane glycoprotein E1. J. Virol. **62:**8–11.
11. **Cinatl, J., B. Morgenstern, G. Bauer, P. Chandra, H. Rabenau, and H. W. Doerr.** 2003. Treatment of SARS with human interferons. Lancet **362:**293–294.
12. **de Veer, M. J., M. Holko, M. Frevel, E. Walker, S. Der, J. M. Paranjape, R. H. Silverman, and B. R. Williams.** 2001. Functional classification of interferon-stimulated genes identified using microarrays. J. Leukoc. Biol. **69:**912–920.
13. **Deonarain, R., A. Alcami, M. Alexiou, M. J. Dallman, D. R. Gewert, and A. C. Porter.** 2000. Impaired antiviral response and alpha/β interferon induction in mice lacking beta interferon. J. Virol. **74:**3404–3409.
14. **Ding, Y., H. Wang, H. Shen, Z. Li, J. Geng, H. Han, J. Cai, X. Li, W. Kang, D. Weng, Y. Lu, D. Wu, L. He, and K. Yao.** 2003. The clinical pathology of severe acute respiratory syndrome (SARS): a report from China. J. Pathol. **200:**282–289.
15. **Drosten, C., S. Gunther, W. Preiser, S. van der Werf, H. R. Brodt, S. Becker, H. Rabenau, M. Panning, L. Kolesnikova, R. A. Fouchier, A. Berger, A. M. Burguiere, J. Cinatl, M. Eickmann, N. Escriou, K. Grywna, S. Kramme, J. C. Manuguerra, S. Muller, V. Rickerts, M. Sturmer, S. Vieth, H. D. Klenk, A. D. Osterhaus, H. Schmitz, and H. W. Doerr.** 2003. Identification of a novel coronavirus in patients with severe acute respiratory syndrome. N. Engl. J. Med. **348:**1967–1976.
16. **Erlandsson, L., R. Blumenthal, M. L. Eloranta, H. Engel, G. Alm, S. Weiss, and T. Leanderson.** 1998. Interferon-beta is required for interferon-alpha production in mouse fibroblasts. Curr. Biol. **8:**223–226.
17. **Fitzgerald, K. A., S. M. McWhirter, K. L. Faia, D. C. Rowe, E. Latz, D. T. Golenbock, A. J. Coyle, S. M. Liao, and T. Maniatis.** 2003. IKKepsilon and

TBK1 are essential components of the IRF3 signaling pathway. Nat. Immunol. **4:**491–496.
18. **Fouchier, R. A., T. Kuiken, M. Schutten, G. van Amerongen, G. J. van Doornum, B. G. van den Hoogen, M. Peiris, W. Lim, K. Stohr, and A. D. Osterhaus.** 2003. Aetiology: Koch's postulates fulfilled for SARS virus. Nature **423:**240.
19. **Fridell, R. A., H. P. Bogerd, and B. R. Cullen.** 1996. Nuclear export of late HIV-1 mRNAs occurs via a cellular protein export pathway. Proc. Natl. Acad. Sci. USA **93:**4421–4424.
20. **Fuchizaki, U., S. Kaneko, Y. Nakamoto, Y. Sugiyama, K. Imagawa, M. Kikuchi, and K. Kobayashi.** 2003. Synergistic antiviral effect of a combination of mouse interferon-alpha and interferon-gamma on mouse hepatitis virus. J. Med. Virol. **69:**188–194.
21. **Garcia-Sastre, A.** 2001. Inhibition of interferon-mediated antiviral responses by Influenza A viruses and other negative-strand RNA viruses. Virology **279:**375–384.
22. **Garcia-Sastre, A., A. Egorov, D. Matassov, S. Brandt, D. E. Levy, J. E. Durbin, P. Palese, and T. Muster.** 1998. Influenza A virus lacking the NS1 gene replicates in interferon-deficient systems. Virology **252:**324–330.
23. **Goodbourn, S., L. Didcock, and R. E. Randall.** 2000. Interferons: cell signalling, immune modulation, antiviral response and virus countermeasures. J. Gen. Virol. **81:**2341–2364.
24. **Haagmans, B. L., T. Kuiken, B. E. Martina, R. A. Fouchier, G. F. Rimmelzwaan, G. Van Amerongen, D. Van Riel, T. De Jong, S. Itamura, K. H. Chan, M. Tashiro, and A. D. Osterhaus.** 2004. Pegylated interferon-alpha protects type 1 pneumocytes against SARS coronavirus infection in macaques. Nat. Med. **10:**290–293.
25. **Hagmaier, K., S. Jennings, J. Buse, F. Weber, and G. Kochs.** 2003. Novel gene product of thogoto virus segment 6 codes for an interferon antagonist. J. Virol. **77:**2747–2752.
26. **He, B., R. G. Paterson, N. Stock, J. E. Durbin, R. K. Durbin, S. Goodbourn, R. E. Randall, and R. A. Lamb.** 2002. Recovery of paramyxovirus simian virus 5 with a V protein lacking the conserved cysteine-rich domain: the multifunctional v protein blocks both interferon-beta induction and interferon signaling. Virology **303:**15–32.
27. **Hiscott, J., P. Pitha, P. Genin, H. Nguyen, C. Heylbroeck, Y. Mamane, M. Algarte, and R. Lin.** 1999. Triggering the interferon response: the role of IRF-3 transcription factor. J. Interferon Cytokine Res. **19:**1–13.
28. **Imani, F., and B. L. Jacobs.** 1988. Inhibitory activity for the interferon-induced protein kinase is associated with the reovirus serotype 1 sigma 3 protein. Proc. Natl. Acad. Sci. USA **85:**7887–7891.
29. **Iwamura, T., M. Yoneyama, K. Yamaguchi, W. Suhara, W. Mori, K. Shiota, Y. Okabe, H. Namiki, and T. Fujita.** 2001. Induction of IRF-3/-7 kinase and NF-kappaB in response to double-stranded RNA and virus infection: common and unique pathways. Genes Cells **6:**375–388.
30. **Juang, Y. T., W. Lowther, M. Kellum, W. C. Au, R. Lin, J. Hiscott, and P. M. Pitha.** 1998. Primary activation of interferon A and interferon B gene transcription by interferon regulatory factor 3. Proc. Natl. Acad. Sci. USA **95:**9837–9842.
31. **Kawamoto, S., K. Oritani, H. Asada, I. Takahashi, J. Ishikawa, H. Yoshida, M. Yamada, N. Ishida, H. Ujiie, H. Masaie, Y. Tomiyama, and Y. Matsuzawa.** 2003. Antiviral activity of limitin against encephalomyocarditis virus, herpes simplex virus, and mouse hepatitis virus: diverse requirements by limitin and alpha interferon for interferon regulatory factor 1. J. Virol. **77:**9622–9631.
32. **Kohl, A., R. F. Clayton, F. Weber, A. Bridgen, R. E. Randall, and R. M. Elliott.** 2003. Bunyamwera virus nonstructural protein NSs counteracts interferon regulatory factor 3-mediated induction of early cell death. J. Virol. **77:**7999–8008.
33. **Ksiazek, T. G., D. Erdman, C. S. Goldsmith, S. R. Zaki, T. Peret, S. Emery, S. Tong, C. Urbani, J. A. Comer, W. Lim, P. E. Rollin, S. F. Dowell, A. E. Ling, C. D. Humphrey, W. J. Shieh, J. Guarner, C. D. Paddock, P. Rota, B. Fields, J. DeRisi, J. Y. Yang, N. Cox, J. M. Hughes, J. W. LeDuc, W. J. Bellini, and L. J. Anderson.** 2003. A novel coronavirus associated with severe acute respiratory syndrome. N. Engl. J. Med. **348:**1953–1966.
34. **Kuiken, T., R. A. Fouchier, M. Schutten, G. F. Rimmelzwaan, G. van Amerongen, D. van Riel, J. D. Laman, T. de Jong, G. van Doornum, W. Lim, A. E. Ling, P. K. Chan, J. S. Tam, M. C. Zambon, R. Gopal, C. Drosten, S. van der Werf, N. Escriou, J. C. Manuguerra, K. Stohr, J. S. Peiris, and A. D. Osterhaus.** 2003. Newly discovered coronavirus as the primary cause of severe acute respiratory syndrome. Lancet **362:**263–270.
35. **Kumar, K. P., K. M. McBride, B. K. Weaver, C. Dingwall, and N. C. Reich.** 2000. Regulated nuclear-cytoplasmic localization of interferon regulatory factor 3, a subunit of double-stranded RNA-activated factor 1. Mol. Cell. Biol. **20:**4159–4168.
36. **Le May, N., S. Dubaele, L. P. De Santis, A. Billecocq, M. Bouloy, and J. M. Egly.** 2004. TFIIH transcription factor, a target for the Rift Valley hemorrhagic fever virus. Cell **116:**541–550.
37. **Levy, D. E., and A. Garcia-Sastre.** 2001. The virus battles: IFN induction of the antiviral state and mechanisms of viral evasion. Cytokine Growth Factor Rev. **12:**143–156.
38. **Li, M., H. Lee, J. Guo, F. Neipel, B. Fleckenstein, K. Ozato, and J. U. Jung.** 1998. Kaposi's sarcoma-associated herpesvirus viral interferon regulatory factor. J. Virol. **72:**5433–5440.
39. **Lin, R., P. Genin, Y. Mamane, and J. Hiscott.** 2000. Selective DNA binding and association with the CREB binding protein coactivator contribute to differential activation of alpha/beta interferon genes by interferon regulatory factors 3 and 7. Mol. Cell. Biol. **20:**6342–6353.
40. **Lin, R., C. Heylbroeck, P. M. Pitha, and J. Hiscott.** 1998. Virus-dependent phosphorylation of the IRF-3 transcription factor regulates nuclear translocation, transactivation potential, and proteasome-mediated degradation. Mol. Cell. Biol. **18:**2986–2996.
41. **Loutfy, M. R., L. M. Blatt, K. A. Siminovitch, S. Ward, B. Wolff, H. Lho, D. H. Pham, H. Deif, E. A. LaMere, M. Chang, K. C. Kain, G. A. Farcas, P. Ferguson, M. Latchford, G. Levy, J. W. Dennis, E. K. Lai, and E. N. Fish.** 2003. Interferon alfacon-1 plus corticosteroids in severe acute respiratory syndrome: a preliminary study. JAMA **290:**3222–3228.
42. **Lu, Y., M. Wambach, M. G. Katze, and R. M. Krug.** 1995. Binding of the influenza virus NS1 protein to double-stranded RNA inhibits the activation of the protein kinase that phosphorylates the eIF-2 translation initiation factor. Virology **214:**222–228.
43. **Lubyova, B., and P. M. Pitha.** 2000. Characterization of a novel human herpesvirus 8-encoded protein, vIRF-3, that shows homology to viral and cellular interferon regulatory factors. J. Virol. **74:**8194–8201.
44. **Marie, I., J. E. Durbin, and D. E. Levy.** 1998. Differential viral induction of distinct interferon-alpha genes by positive feedback through interferon regulatory factor-7. EMBO J. **17:**6660–6669.
45. **Mori, M., M. Yoneyama, T. Ito, K. Takahashi, F. Inagaki, and T. Fujita.** 2004. Identification of ser-386 of interferon regulatory factor 3 as critical target for inducible phosphorylation that determines activation. J. Biol. Chem. **279:**9698–9702.
46. **Pei, J., M. J. Sekellick, P. I. Marcus, I. S. Choi, and E. W. Collisson.** 2001. Chicken interferon type I inhibits infectious bronchitis virus replication and associated respiratory illness. J. Interferon Cytokine Res. **21:**1071–1077.
47. **Peiris, J. S., C. M. Chu, V. C. Cheng, K. S. Chan, I. F. Hung, L. L. Poon, K. I. Law, B. S. Tang, T. Y. Hon, C. S. Chan, K. H. Chan, J. S. Ng, B. J. Zheng, W. L. Ng, R. W. Lai, Y. Guan, and K. Y. Yuen.** 2003. Clinical progression and viral load in a community outbreak of coronavirus-associated SARS pneumonia: a prospective study. Lancet **361:**1767–1772.
48. **Peiris, J. S., S. T. Lai, L. L. Poon, Y. Guan, L. Y. Yam, W. Lim, J. Nicholls, W. K. Yee, W. W. Yan, M. T. Cheung, V. C. Cheng, K. H. Chan, D. N. Tsang, R. W. Yung, T. K. Ng, and K. Y. Yuen.** 2003. Coronavirus as a possible cause of severe acute respiratory syndrome. Lancet **361:**1319–1325.
49. **Peiris, J. S., K. Y. Yuen, A. D. Osterhaus, and K. Stohr.** 2003. The severe acute respiratory syndrome. N. Engl. J. Med. **349:**2431–2441.
50. **Poole, E., B. He, R. A. Lamb, R. E. Randall, and S. Goodbourn.** 2002. The v proteins of simian virus 5 and other paramyxoviruses inhibit induction of interferon-beta. Virology **303:**33–46.
51. **Ronco, L. V., A. Y. Karpova, M. Vidal, and P. M. Howley.** 1998. Human papillomavirus 16 E6 oncoprotein binds to interferon regulatory factor-3 and inhibits its transcriptional activity. Genes Dev. **12:**2061–2072.
52. **Ruggli, N., J. D. Tratschin, M. Schweizer, K. C. McCullough, M. A. Hofmann, and A. Summerfield.** 2003. Classical swine fever virus interferes with cellular antiviral defense: evidence for a novel function of N(pro). J. Virol. **77:**7645–7654.
53. **Samuel, C. E.** 2001. Antiviral actions of interferons. Clin. Microbiol. Rev. **4:**778–809.
54. **Schafer, S. L., R. Lin, P. A. Moore, J. Hiscott, and P. M. Pitha.** 1998. Regulation of type I interferon gene expression by interferon regulatory factor-3. J. Biol. Chem. **273:**2714–2720.
55. **Schweizer, M., and E. Peterhans.** 2001. Noncytopathic bovine viral diarrhea virus inhibits double-stranded RNA-induced apoptosis and interferon synthesis. J. Virol. **75:**4692–4698.
56. **Servant, M. J., N. Grandvaux, B. R. tenOever, D. Duguay, R. Lin, and J. Hiscott.** 2003. Identification of the minimal phosphoacceptor site required for in vivo activation of interferon regulatory factor 3 in response to virus and double-stranded RNA. J. Biol. Chem. **278:**9441–9447.
57. **Servant, M. J., B. ten Oever, C. LePage, L. Conti, S. Gessani, I. Julkunen, R. Lin, and J. Hiscott.** 2001. Identification of distinct signaling pathways leading to the phosphorylation of interferon regulatory factor 3. J. Biol. Chem. **276:**355–363.
58. **Sharma, S., B. R. TenOever, N. Grandvaux, G. P. Zhou, R. Lin, and J. Hiscott.** 2003. Triggering the interferon antiviral response through an IKK-related pathway. Science **17:**17.
59. **Spiegel, M., A. Pichlmair, E. Mühlberger, O. Haller, and F. Weber.** 2004. The antiviral effect of interferon-beta against SARS-coronavirus is not mediated by MxA. J. Clin. Virol. **30:**211–213.
60. **Stark, G. R., I. M. Kerr, B. R. Williams, R. H. Silverman, and R. D. Schreiber.** 1998. How cells respond to interferons. Annu. Rev. Biochem. **67:**227–264.
61. **Suhara, W., M. Yoneyama, I. Kitabayashi, and T. Fujita.** 2002. Direct involvement of CREB-binding protein/p300 in sequence-specific DNA binding of virus-activated interferon regulatory factor-3 holocomplex. J. Biol. Chem. **277:**22304–22313.

62. **Sun, H. Y., C. T. Fang, J. T. Wang, Y. C. Chen, and S. C. Chang.** 2003. Treatment of severe acute respiratory syndrome in health-care workers. Lancet **362:**2025–2026.
63. **Thomas, D., G. Blakqori, V. Wagner, M. Banholzer, N. Kessler, R. M. Elliott, O. Haller, and F. Weber.** 2004. Inhibition of RNA polymerase II phosphorylation by a viral interferon antagonist. J. Biol. Chem. **279:**31471–31477.
64. **van Pesch, V., O. van Eyll, and T. Michiels.** 2001. The leader protein of Theiler's virus inhibits immediate-early alpha/beta interferon production. J. Virol. **75:**7811–7817.
65. **Wathelet, M. G., C. H. Lin, B. S. Parekh, L. V. Ronco, P. M. Howley, and T. Maniatis.** 1998. Virus infection induces the assembly of coordinately activated transcription factors on the IFN-β enhancer in vivo. Mol. Cell **1:**507–518.
66. **Weaver, B. K., K. P. Kumar, and N. C. Reich.** 1998. Interferon regulatory factor 3 and CREB-binding protein/p300 are subunits of double-stranded RNA-activated transcription factor DRAF1. Mol. Cell. Biol. **18:**1359–1368.
67. **Weber, F., A. Bridgen, J. K. Fazakerley, H. Streitenfeld, R. E. Randall, and R. M. Elliott.** 2002. Bunyamwera bunyavirus nonstructural protein NSs counteracts the induction of alpha/beta interferon. J. Virol. **76:**7949–7955.
68. **Weber, F., G. Kochs, O. Haller, and P. Staeheli.** 2003. Viral evasion of the interferon system: old viruses, new tricks. J. Interferon Cytokine Res. **23:** 209–213.
69. **World Health Organization.** 2003. Summary table of SARS cases by country, 1 November 2002–26 September 2003. http://www.who.int/csr/sars/country/table2003_09_23/en/.
70. **Xiang, Y., R. C. Condit, S. Vijaysri, B. Jacobs, B. R. Williams, and R. H. Silverman.** 2002. Blockade of interferon induction and action by the E3L double-stranded RNA binding proteins of vaccinia virus. J. Virol. **76:**5251–5259.
71. **Yoneyama, M., M. Kikuchi, T. Natsukawa, N. Shinobu, T. Imaizumi, M. Miyagishi, K. Taira, S. Akira, and T. Fujita.** 2004. The RNA helicase RIG-I has an essential function in double-stranded RNA-induced innate antiviral responses. Nat. Immunol. **5:**730–737.
72. **Yoneyama, M., W. Suhara, Y. Fukuhara, M. Fukuda, E. Nishida, and T. Fujita.** 1998. Direct triggering of the type I interferon system by virus infection: activation of a transcription factor complex containing IRF-3 and CBP/p300. EMBO J. **17:**1087–1095.
73. **Zimring, J. C., S. Goodbourn, and M. K. Offermann.** 1998. Human herpesvirus 8 encodes an interferon regulatory factor (IRF) homolog that represses IRF-1-mediated transcription. J. Virol. **72:**701–707.
74. **Zoll, J., W. J. Melchers, J. M. Galama, and F. J. van Kuppeveld.** 2002. The mengovirus leader protein suppresses alpha/beta interferon production by inhibition of the iron/ferritin-mediated activation of NF-κB. J. Virol. **76**: 9664–9672.